AUTONOMOUS AEROBRAKING AT MARS

Jill L. Hanna
NASA Langley Research Center
j.l.hanna@larc.nasa.gov
Robert Tolson, George Washington University
Alicia Dwyer Cianciolo and John Dec, NASA Langley Research Center

Abstract

Aerobraking has become a proven approach for orbital missions at Mars. A launch of a 1000 kg class spacecraft on a Delta class booster saves 90% of the post-MOI fuel otherwise required to circularize the orbit. In 1997, Mars Global Surveyor demonstrated the feasibility and Mars 2001 Odyssey completed a nearly trouble free aerobraking phase in January 2002. In 2006, Mars Reconnaissance Orbiter will also utilize aerobraking. From the flight operations standpoint, however, aerobraking is labor intensive and high risk due to the large density variability in the Mars thermosphere. The maximum rate of aerobraking is typically limited by the maximum allowable temperature of the solar array which is the primary drag surface. Prior missions have used a surrogate variable, usually maximum free stream heat flux, as a basis for performing periapsis altitude corridor control maneuvers. This paper provides an adaptive sequential method for operationally relating measured temperatures to heat flux profile characteristics and performing maneuvers based directly on measured temperatures and atmospheric properties derived from the heat flux profiles. Simulations of autonomous aerobraking are performed using Odyssey mission data.

Nomenclature

ρ	atmospheric density, kg/km^3
A	spacecraft aerodynamic reference area, m
a_d	acceleration due to drag, m/s^2
AB	aerobraking
C_d	drag coefficient
e	orbital eccentricity
GM	Mars gravitational constant
h	altitude above reference ellipsoid, km
H	total heat input due to aerobraking, W
H_s	density scale height, km
IMU	Inertial Measurement Unit
m	spacecraft mass, kg
MLI	Multi-Layer Insulation
MOI	Mars Orbit Insertion
MGS	Mars Global Surveyor
q	dynamic pressure
Q	free stream heat flux, W/cm^2
r_p	periapsis altitude, km
SA	solar array
s/c	spacecraft
T	spacecraft temperature, °C
V	spacecraft velocity, km/s

Introduction

Aerobraking (AB) is the utilization of atmospheric drag for beneficial orbit changes. The feasibility of AB was first demonstrated in a planetary mission[1] during the Venus Magellan mission. Magellan AB was performed over about 70 days and 750 orbital passes to reduce the orbital eccentricity from 0.3 to 0.03. The second application was on the Mars Global Surveyor (MGS) where over 850 AB passes[2] reduced the post-MOI period from about 45 hours to about 2 hours, saving an equivalent impulsive ΔV of approximately 1.2 km/s. Mars Odyssey performed over 300 AB passes to reduce the orbital period from 18 hours to about 2 hours[3] saving more than 1.1 km/s in ΔV. For both MGS and Odyssey, aerobraking was essential for mission success.

Since the solar arrays (SA) are the primary drag surfaces, SA temperature is likely to be the limiting criteria for aerobraking. Consequently, the large systematic and random orbit to orbit atmospheric variations discovered during MGS[4] and Odyssey[5] led to labor intensive operations. For both missions, the plan was to use maximum free stream heat flux (Q_{max}) on each orbit to provide the information to decide whether periapsis altitude should be raised or lowered for subsequent passes. Because of the damaged SA, MGS AB was actually limited by maximum dynamic pressure during each pass equivalent to about one half of the maximum heating limit. The Odyssey periapsis altitude corridor was defined in terms of maximum free stream heat flux. Corridor bounds were obtained by pre-flight thermal analyses to relate Q_{max} to SA temperatures. The SA were flight qualified to 195^{o}C. Even though both missions had temperature sensors on the SA, the sensors were not necessarily located near regions where either high heat flux or high temperatures were expected. In flight analyses[6] were performed comparing measured temperatures with thermal model results to assure corridor integrity. Maximum temperatures reached on the SA are functions of the initial temperature at the

beginning of AB, the maximum heat flux and the heat flux profile during the pass.

Reducing the operational cost and risk of AB can only be done with an autonomous system that provides confidence that SA temperatures will not exceed flight qualification or flight allowable limits. Studies have been performed[7] of various modes of autonomous AB based on utilizing the maximum heat flux corridor approach. Feasibility of a simple approach to estimate change in orbital period based on accelerometer measurements was demonstrated on Odyssey.[8] This paper provides an adaptive, sequential method for operationally relating measured temperatures to heat flux profile characteristics and performing maneuvers based directly on measured temperatures and atmospheric properties derived from the heat flux profiles. The approach is validated using Odyssey mission data.

Mars 2001 Odyssey Aerobraking

Fig. 1 shows the Odyssey spacecraft in the AB configuration. To provide a view of the bus components, the MLI that covers the bus is not shown. Two IMU's are located on the upper deck and provide the accelerometer data that will be used to characterize the atmosphere density profile. There are three solar panels and the center panel is latched to the bus during aerobraking. The arrays have an aluminum honeycomb core and graphite composite face sheets. Four

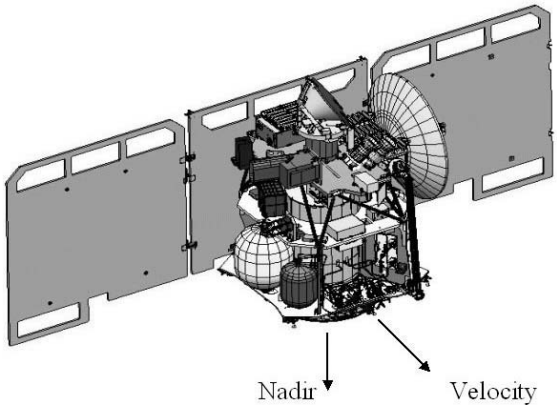

Figure 1. Odyssey in aerobraking configuration

temperature sensors are located on the two exposed solar panels with one on the front and back of each panel. T1 and T4 are located on the front surface, i.e. the surface directly exposed to the free stream, and T2 and T5 are on the back surface where the solar cells are attached. T1 and T4 are located next to the SA cutouts, on the 'handle' looking structures and have significantly different thermal properties than the main area of the SA. During the AB pass, the flow is well into the free molecular-continuum transition region[9] so that the maximum aerodynamic heat flux occurs near the edges of the panel. The edges were consequently wrapped with a MLI to mitigate the effects of this higher heating and the MLI covers T1 and T4. A fifth thermocouple, T3, was located on the cell side behind the s/c bus and provided no data of interest for AB.

Fig. 2 shows the four measured temperatures and the free stream heat flux for orbit 106, which had the highest heat flux (0.52 W/cm^2) during the entire mission. The heat flux is based on atmospheric density derived from the accelerometer data.[5] Prior to the beginning of an AB pass, the SA are facing the sun and have generally reached a radiative equilibrium temperature.

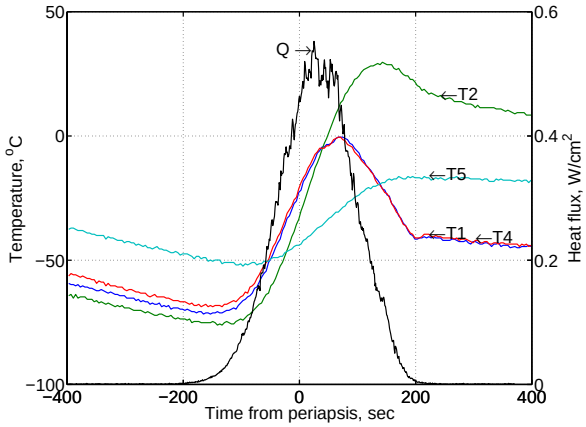

Figure 2. Measured temperature and heat flux, orbit 106.

To begin the AB sequence, the SA are latched to the bus and the s/c is oriented to face into the free stream flow. Until aerodynamic heating begins, the array temperature generally decreases due to radiative cooling. Being on the front face, T1 and T4 begin to increase in temperature before the back face temperatures. For orbit 106, maximum front face temperatures occur at the time that the heat flux begins to decrease, while the back face maximum occurs about 100 seconds later. Many Odyssey and MGS orbits did not provide the nearly symmetric, unimodal heat flux profile shown here. The Mars thermosphere density can be highly variable on latitudinal and longitudinal scales of 20 km.[5] However, SA thermal transfer processes tend to damp such fluctuations and maximum front face temperatures are nearly in phase with the maximum of the 30 second average of Q. At the end of the atmospheric pass, the arrays continue to cool to the end of the AB sequence.

Because of the poor strategic location of the sensors, it is impossible to determine the maximum temperature reached on the arrays without resorting to thermal modeling. The results of one such modeling effort are shown in Fig. 3. The temperatures are shown a

short time after maximum heat flux. The effects of the MLI on the perimeter of the arrays are clearly evident in the lower temperatures and the shadowing due to the high gain antenna is also evident. Maximum front side temperature is predicted[6] to have reached 135°C. Comparing temperatures throughout the AB pass shows that the difference between model and measured temperatures for T1, T2, and T4 were within 10°C, while T5 differences were as great as 20°C.

During operations, Q_{max} was used as the surrogate variable for making maneuver decisions to determine whether to increase atmospheric density and hence Q_{max} by lowering periapsis altitude or conversely.[3] The relationship between Q_{max} and maximum temperature was determined pre-flight and tuned slightly once AB began. A cartoon of this relationship is shown in Fig. 4.

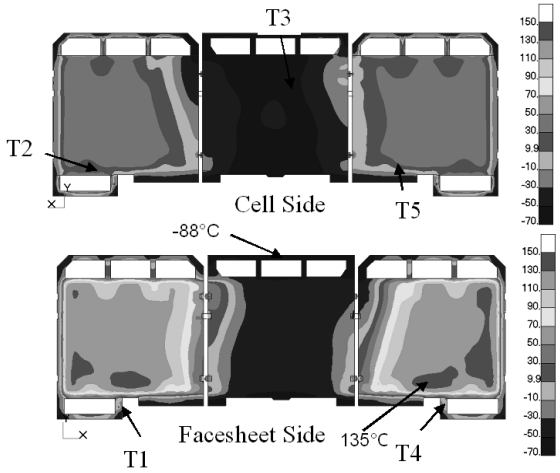

Figure 3. Solar array face sheet temperatures at time of maximum face sheet temperature, orbit 106.

The actual AB limit is the 195°C vertical qualification line. The flight allowable was set at 175°C to provide a safety margin. The conversion to Q_{max} requires assuming a heating profile. A Gaussian looking symmetric, unimodal distribution was selected as representative of the traditional isothermal atmosphere. The width of the profile varied through out the mission, getting longer as the eccentricity of the orbit decreased and the AB duration became longer. Fig. 4 shows the relationship for the high eccentricity orbits that occurred soon after MOI. Based on the thermal analyses, the Q_{max} corresponding to the qualification limit was set at 0.65 W/cm^2 and the flight allowable was set at 0.54 W/cm^2. To account for the 30-40% 1-σ orbit to orbit variability of the Mars atmosphere, an additional 80% to 100% margin was used, thereby setting the upper corridor boundary at about 0.32 W/cm^2 resulting in a predicted maximum SA temperature of 80°C. The lower boundary is set by other mission considerations such as number of maneuvers required to stay in the corridor and orbit geometry at the end of the AB phase. Also shown on the figure is the black body radiation heat flux as a function of the SA temperature. Note that radiative cooling is a small fraction of the aerodynamic heating over the AB range.

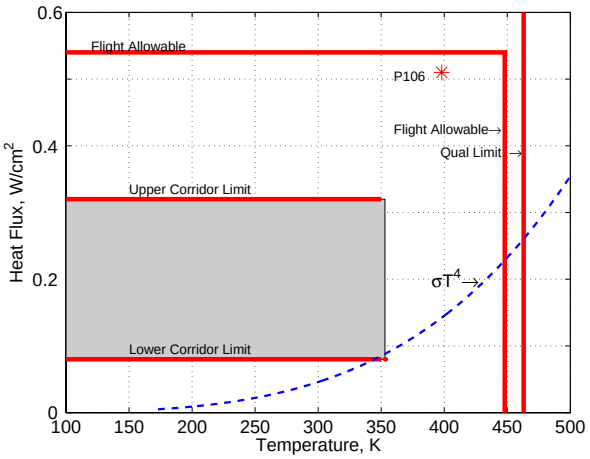

Figure 4. Aerobraking corridor and solar array temperature limits.

The actual corridor and flight results are shown in Fig. 5. The Q_{max} for each orbit is shown as a function of the orbital period. The objective of aerobraking was to reduce the period from the initial 18 hours to about 2 hours. The circles locate periapsis altitude maneuvers.

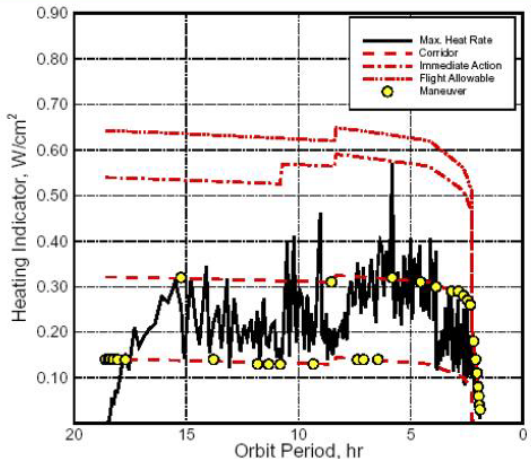

Figure 5. Odyssey aerobraking heat rate versus orbital period.

The allowable limit decreases as the AB pass gets longer and was adjusted upward as confidence grew and conservatism in the thermal model was reduced. For orbital periods below about 4 hours, orbit life time became the limiting factor rather than heating. During

the main AB phase, only 11 maneuvers were required to maintain the mission in the corridor. As an indication of the variability of the Mars thermosphere, note that orbit 106 had a Q_{max} about double adjacent orbits at approximately the same periapsis altitude.

Outline of Approach

It is assumed that SA temperature is the limiting factor in determining the maximum rate of aerobraking and that temperature measurements are available from which the maximum temperature can be estimated with confidence. The deficiency in the Odyssey sensor locations has been recognized and future missions will more than likely locate sensors more strategically. For algorithm demonstration, thermal model derived maximum temperature will be used. The model has been tuned over the entire mission[6] and average difference in peak temperatures at the relevant sensors was 3.4°C and the standard deviation of the difference throughout an AB pass, averaged over all passes, was 5°C.

The only other data used in the algorithm is the traditionally available accelerometer data from the IMU. These data directly measure the acceleration due to drag (a_d). Dynamic pressure, $q=1/2\rho V^2$, can be calculated from the equation of motion, $ma_d=qC_dA$, where m is the s/c mass, ρ is the atmospheric density, C_d is the drag coefficient, A is the s/c reference area. During a single AB pass, the spacecraft velocity, V, varies from the value at periapsis by less than one percent. The drag coefficient is a weak function of atmospheric density and varies from 2.2 in the upper atmosphere to about 1.8 at periapsis for orbit 106. For autonomous operations, a short interpolation table of C_d vs qC_d would be stored onboard to provide direct determination of C_d and then q. The free stream heat flux is

$$Q=1/2\rho V^3 = qV \qquad (1)$$

and the total heat input, H, is the integral of Q over the AB pass. In the algorithm, the accelerometer data will be used to calculate the total heat input during the pass, the maximum heat flux, and the effective scale height of the atmosphere for heating. The coefficients of a linear relation between maximum temperature and the first two parameters are updated in a sequential manner after each pass and used to predict maximum temperature on subsequent passes. Maneuver decisions are then based directly on predicted maximum temperature.

The use of these two variables in the regression is based on the following simplified physical rational. For the initial high eccentricity orbits, the significant heating part of the AB pass is "short" compared to the time for conduction to transfer the heat from the face sheet through the SA. The heat input acts like an impulse so the face sheet temperature increase is primarily due to the total heat input. For the low eccentricity orbits, the AB duration is "long" compared to the time for conduction through the SA to take place, so that the temperature increase is determined primarily by the maximum heat flux. As the mission evolves, the relative importance of the two terms will change. Another way of thinking of these two parameters is that the total heat input is the maximum heat flux times an "effective" pulse width. So, the regression is equivalently using the maximum heat flux and effective pulse width as parameters.

As an example of the utilization of the approach, consider Fig. 6. This figure shows the measured temperature at T4 during the entire main AB phase of the mission. The lower curve shows the temperature just prior to the beginning of heating and the upper curve provides the maximum temperature during the pass. The minimum temperature varies slowly because the orbit

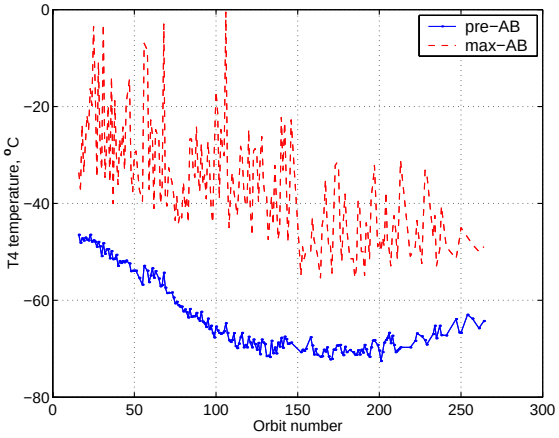

Figure 6. Minimum and maximum temperatures at T4 during the Odyssey mission.

geometry and mission sequence only change slightly from orbit to orbit. The variability in the maximum temperature is primarily due to the orbit to orbit variation in the atmospheric density.

Fig 7 provides the results of a linear regression analyses. The upper panel provides a plot of the maximum temperature increase at T4 due to AB heating, i.e. the difference in the two sets of data in Fig. 6, versus the maximum heating rate during each orbit. The line represents the least square linear fit to these data. The coefficients of the model are shown in the figure along with the RMS residual after the fit, which is 3.45°C. The second frame provides similar results with the regression against the total heat input, H, with a resulting residual of 3.26°C. The final frame shows the residuals when both parameters are included in the solution. The residual has

now been reduce to 1.8ºC 1-σ. So using Q_{max} and H as

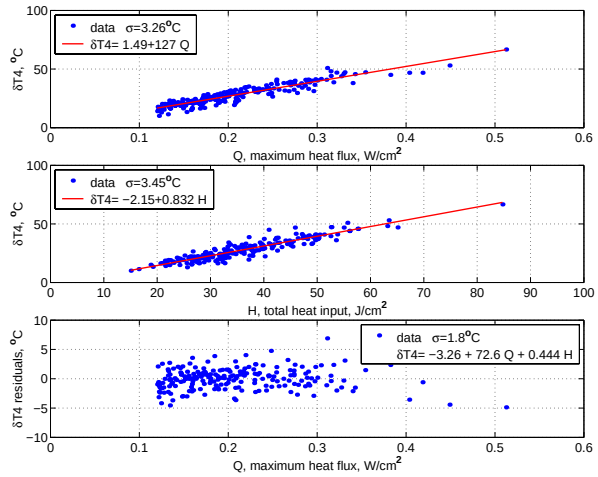

Figure 7. Least squares solutions for T4 temperature increase during main aerobraking phase.

regression parameters appears to be adequate for temperature prediction over the entire Odyssey mission. Alternatively, either parameter could be used separately and still result in less than 4ºC 1-σ prediction error. The latter approach will be used here to provide more direct comparison with the Odyssey maneuver strategy. For finite memory filters, spanning less than 40 orbits, only 1 parameter is recommended because of the high correlation between Q_{max} and H for orbits with similar eccentricities.

After the temperature increases for future orbits are predicted, the decision to perform a maneuver must be made. From Eq 1, Q_{max} is proportional to the maximum density, so that, if a maneuver is required, the magnitude of the maneuver to raise or lower subsequent periapsis altitudes will depend on the assumed density variation with altitude. It is generally adequate to assume that density varies exponentially with altitude, h, so that

$$\rho(h)=\rho\,(h_o)\exp(-(h-h_o)/H_s) \qquad (2)$$

where H_s is the density scale height and h_o is the reference altitude generally taken to be the current periapsis altitude. During MGS and Odyssey operations, the density at periapsis and H_s were determined by least squares solutions to Eq. 2. The results for Odyssey are shown at the top of Fig. 8. An alternate approach is to use Q_{max} and H directly and some approximations[10] to derive the relation

$$H_s = (H/\,Q_{max})^2\, e\, GM/(2\pi\, r_p^{\,2}) \qquad (3)$$

where e is the orbital eccentricity, GM is the Mars gravity constant and r_p is the periapsis radius. Scale heights derived from Eq. 3 are shown in the middle panel of Fig. 8. The large orbit to orbit variability and the large differences between the two approaches result from large, nearly random global and local variations[5,11] in the Mars thermosphere. Even with these large differences, the 7 point running means, in the lowest panel, are within 10%. Consequently a low order finite memory filter would be used in an autonomous system. Each method for determining H_s has advantages and disadvantages and the selection would depend on the particular application.

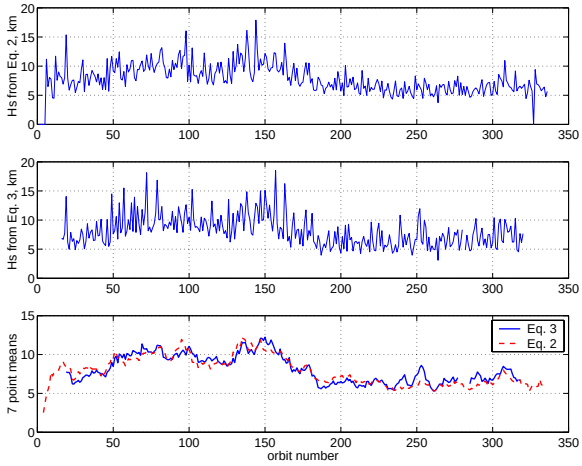

Figure 8. Comparison of two methods of determining density scale height.

Finally if Q_n is the maximum heat flux on orbit n at periapsis altitude h_n and the target heat flux for the next orbit is Q_{n+1}, then the maneuver would be targeted for an altitude of

$$h_{n+1} = h_n - H_s \log(Q_{n+1}/Q_n) \qquad (4)$$

The maneuver would be performed at the apoapsis between the n-th and n-th+1 aerobraking passes. This is, of course, a simplification of the operational or autonomous aerobraking process that would include precision integrated trajectories and perhaps other considerations.

In summary, the approach assumes that face sheet temperature, T_1, just prior to the beginning of aerobraking and the maximum face sheet temperature, $T_{max,}$ for each AB pass can be estimated from direct measurements of face sheet temperatures. Secondly, Q_{max} and H are determined from drag as measured by accelerometers. A sequential filter is applied to the temperature increase, $\Delta T = T_{max,} - T_1$, due to AB heating to update model coefficients relating ΔT to Q_{max} and/or

H. A finite memory filter is used to estimate T_1 as a function of orbit number. Except in unusual situations, assuming T_1 is linear with orbit number over 7 to 10 orbits is adequate. These two models, along with an integration of the orbit forward in time to calculate subsequent values of Q_{max} and/or H, are used to predict T_{max} on future orbits. A maneuver strategy is then implemented based on these projections.

Application to Odyssey

Unfortunately there were no measurements of maximum face sheet temperatures on Odyssey. The T4 measurement site (Fig. 3) is the closest to the maximum temperature locations. Consequently, for the simulation maximum temperatures derived from a thermal model[6] will be used to extrapolate the T_{max} and T_1 measured at T4 (Fig. 6) to what would have been the entire face sheet maximum. The results of this extrapolation are shown in Fig 9.

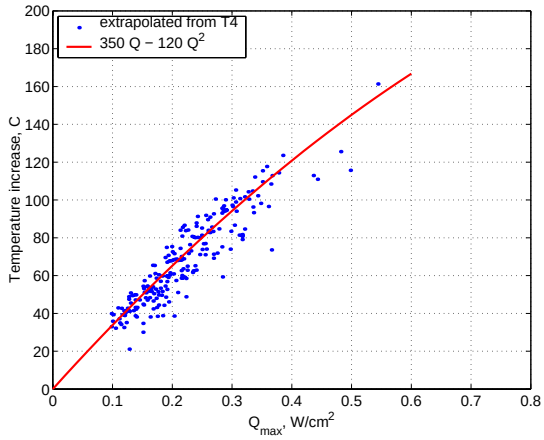

Figure 9. Maximum face sheet temperature increase derived by extrapolating Odyssey measurements.

The points represent the orbits for which thermal analyses were performed to support Odyssey operations. As might be expected, at the lower values of Q_{max} the temperature increase is proportional to Q_{max}, but at the higher values there is a decrease in the slope, perhaps due to the increased importance of heat rejection by radiation. For the simulations, the model line $\Delta T=350Q_{max} - 120Q_{max}^2$ will be used with a random addition of 2° C. The simulation process is the same as previously reported[7] and the underlying atmospheric model[12] was developed for performing Monte Carlo simulations of the Odyssey mission both pre-flight and during operations. Fig. 10 presents the results from a simulation using the Odyssey approach based on a Q_{max} corridor.

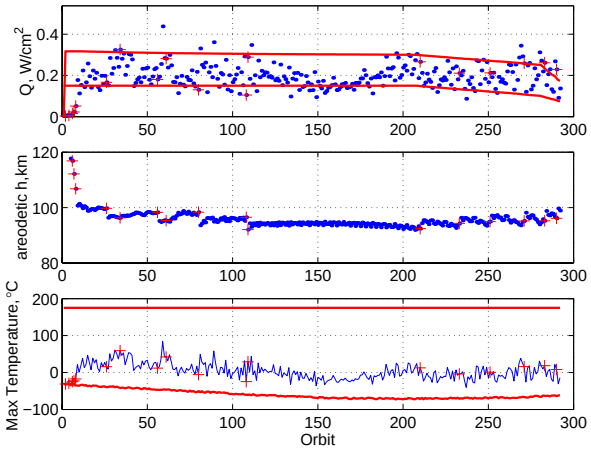

Figure 10. Simulation of Odyssey mission using Q_{max} corridor.

This particular simulation is similar to the actual mission shown in Fig. 5. The simulation took 77 days and 292 orbits while the mission required 75 days and 336 orbits. The simulation required 18 maneuvers for a total maneuver ΔV of 4.2 m/s while the mission, including walk-in and endgame but excluding the final aerobraking termination maneuver, performed 32 maneuvers with ΔV=26.7 m/s. Note that the predicted maximum face sheet temperature of 84°C is well below the flight allowable. For Odyssey the maximum predicted face sheet temperature was 134°C and occurred on orbit 106 at Q_{max}=0.52 W/cm^2 The simulation reached a minimum altitude of 92 km and the mission was at a minimum of 95 km on orbit 105.

In each simulation using a maximum temperature corridor, the maximum temperature for three subsequent orbits was calculated based on the model shown in Fig 9. The mean of these temperatures was compared to the temperature corridor and the decision to make a periapsis raise or lower maneuver was based on the location of this mean within the corridor. The top of the temperature corridor was set at 50%, 62.5%, or 75% of the expected temperature increase due to AB heating. Using the relationship between Q_{max} and T_{max} derived from the recursive filter on past orbits, this upper boundary is converted to an equivalent upper boundary on Q_{max}. The lower boundary is set 0.17 W/cm^2 below the upper boundary. This width is the same as the initial corridor width in the simulation shown in Fig. 10 and primarily determines the number of maneuvers during the mission.

Results for these three cases are shown in Fig 11 and Fig 12. The dashed lines are the calculated corridor. The “walk-in” and ‘walk-out” corridors are the same for all cases. Walk-in is the first 6 to 10 orbits when periapsis altitude is decreased from 150-200 km to about 110 km. Walk-out occurs at the end of the mission when

orbit lifetime becomes the aerobraking constraint and periapsis altitude is increased systematically to maintain at least a 24 hour lifetime. The upper red line in Fig. 12 refers to a constant 175°C flight allowable line. The lower sloped line on each plot represents the minimum temperature of the SA, prior to atmospheric entry for each orbit. These figures show that even for the case where the target temperature increase is 50% of the expected value, the mission duration is reduce to 230 orbits and the maximum temperature is 100° below the flight allowable. The 62.5% case has no orbits that come within 50°C of the flight allowable and the 75% case has a number of orbits within 40°C. The lowest altitude reached in each case are 89, 86 and 84 km respectively. Although insufficient Monte Carlo simulations were performed to produce meaningful statistics, the 75% case may present too much risk of exceeding the flight allowable.

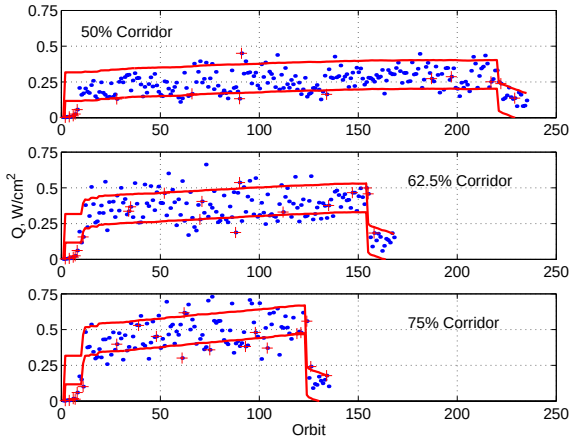

Figure 11. Heat rate results for three maneuver strategies.

Parameters that relate to AB efficiency are summarized in Table 1. The traditional strategy in given in the first row and the proposed T_{max} strategy in the last 3 rows. Each set of numbers is the average of 3 simulations. The ΔV utilization is not significantly different for the various strategies. In fact most of the ΔV is utilized during 'walk out.' The number of maneuvers is also not significantly different. The main advantage of utilizing the T_{max} strategy is the large reductions in the number of AB orbits and the total time for the AB phase of the mission. The former reduces the risk of potential procedural errors associated with each AB pass while increasing the risk of exceeding the flight allowable temperature. Reducing the duration of the AB phase of the mission reduces the operational cost for a non-autonomous mission and reduces the potential for human errors that might occur as mission duration becomes longer. The risk and cost trades can only be made after more analysis for a particular mission.

Table 1. Aerobraking Mission Parameters

% corridor	T_{max}	Total ΔV	Days of AB	Orbits
NA	84	4.2	77	292
0.5	85	3.7	66	236
0.625	130	3.3	47	167
0.75	161	4	38	129

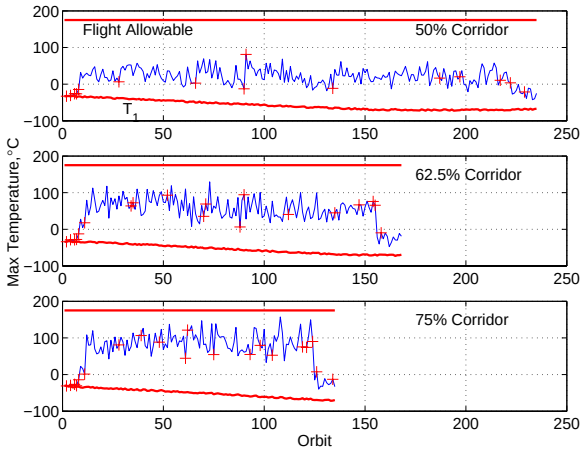

Figure 12. Maximum temperatures for three maneuver strategies.

Concluding Remarks

The proposed method for using direct measurements of solar array maximum temperatures as the basis for the aerobraking maneuver has been developed and evaluated using Odyssey mission simulations. The approach shows the potential to significantly reduce the number of aerobraking orbits and the total time of the AB phase of the mission. The approach relies on measurements of the parameters that define mission failure criteria, i.e. maximum SA temperatures, instead of relying on surrogate variables that appear to add a considerable degree of conservatism.

During the early phases of Odyssey aerobraking, the rate of aerobraking fell significantly behind the design profile[3] due in part to the large atmospheric variability as periapsis latitude precessed through the polar vortex. While periapsis was inside the vortex (approximately orbits 100-150 in Fig 6), atmospheric orbit-to-orbit variability was found to be as low as 10%. This unexpected and beneficial low variability provided the opportunity to aggressively aerobrake and make up the deficit. Note from the figure that had the corridor

been defined in terms of maximum temperature, there would have been no need to depend on the serendipitous occurrence of low variability inside the vortex. The temperature of the SA at the beginning of each AB pass had decreased by 20°C to 25°C from the beginning of the mission. Based on the slope of 350 °/W/cm^2 in Fig. 9, this decrease would have provided an increase in the upper Q_{max} corridor limit of between 0.06 and 0.07 W/cm^2. This amounts to a 20% higher upper limit and would have been adequate to maintain the design aerobraking profile.

For Odyssey, the benefit is due to SA radiative cooling prior to the beginning of AB. There are two main contributors to this cooling. The reorientation to AB attitude generally reduces the solar heat input and this occurs 5 to 10 minutes before entering the atmosphere. To provide increased AB safety margin, increasing this duration could be traded against other mission constraints. The second contributor is the time that solar eclipse occurs relative to the beginning of AB. This is a function of Mars season and the orbit geometry angles. For high inclination initial orbits, periapsis latitude will usually precess toward the nearest pole. If this happens to be a winter pole, solar eclipses will generally occur earlier in the orbit and last longer. Conversely for a summer pole. High inclination orbits resulting from type 1 interplanetary transfers usually start with periapsis LST near or later than 1800 hrs. If periapsis latitude did not precess, the orbital motion of Mars moves periapsis towards earlier times. Odyssey had nearly the optimal situation, a type 1 transfer and periapsis precession toward the winter north pole. Periapsis LST started near 1800 hrs. Mars orbital motion moved periapsis to slightly earlier times but apsidal precession quickly overcame the orbital motion effect, and periapsis LST moved toward midnight and then into the early morning hours.

When surrogate variables like Q_{max} are used, aerobraking is seldom considered in the selection of the post-MOI orbit orientation or interplanetary mission design. The surrogate variable approach deprives the mission and spacecraft designers of an additional degree of freedom for optimizing the mission that could have been provided by directly using the maximum SA temperature in the design.

References

[1]Lyons, D. T., "Aerobraking Magellan: Plan versus reality," Advances in the Astronautical Sciences, Vol. 87, Pt. 2, 1994, pp. 663-680.

[2]Lyons, D. T., et al., "Mars Global Surveyor: Aerobraking Mission Overview," *Journal of Spacecraft and Rockets*, Vol. 36, No 3, 1999, pp. 307-313.

[3] Smith, J. & Bell, J., "2001 Mars Odyssey Aerobraking" AIAA-2002-4532 Astrodynamics Specialist Conference, Monterey, CA, August 5, 2002.

[4]Tolson, R. H., et al., "Application of Accelerometer Data to Mars Global Surveyor Aerobraking Operations," *Journal of Spacecraft and Rockets*, Vol 36, No 3, pp. 323-329, 1999.

[5] Tolson, R.. H., et al., "Applications of Accelerometer Data to Mars Odyssey Aerobraking and Atmospheric Modeling," AIAA Astrodynamics Specialist Conference, Monterey, CA, August 5, 2002

[6]Dec, J., et al., "Thermal Analysis and Correlation of the Mars Odyssey Spacecraft's Solar Array During Aerobraking Operations", AIAA 2002-4536, Astrodynamics Specialist Conference, Monterey, CA, August 5, 2002.

[7]Hanna, J.L. and Tolson, R.H., "Approaches to Autonomous Aerobraking at Mars," AAS/AIAA Astrodynamics Specialist Conference, Quebec City, Canada, July 30-August 2, 2001. AAS 01-387.

[8]Willcockson, W. and Johnson, M., "Mars Odyssey Aerobraking: The First Step Towards Autonomous Aerobraking Operations" 2003 IEEE Aerospace Conference, Big Sky, MT, March 9-14, 2003.

[9]Takashima, N. and Wilmoth, R. G., "Aerodynamics of Mars Odyssey," AIAA-2002-4809, 2002 Atmospheric Flight Mechanics Conference, Monterey, CA, August 5, 2002.

[10]King-Hele, D., "Satellite Orbits in an Atmosphere" Blackie and Son, Ltd, London, 1987.

[11]Tolson, R. H., et al., "Utilization of Mars Global Surveyor Accelerometer Data for Atmospheric Modeling," Astrodynamics 1999, Vol 103, American Astrodynamics Society, 1999.

[12]Dwyer, A. M., et. al., "Development of a Monte Carlo Mars-GRAM Model for Mars 2001 Aerobraking Simulations" Advances in the Astronautical Sciences, Vol. 109, 2001, pp. 1293-1308.